

## Equilibrium conditions and magnetic field rotation at the tangential discontinuity magnetopause

J. De Keyser and M. Roth

Belgian Institute for Space Aeronomy, Brussels

**Abstract.** De Keyser and Roth recently have developed a kinetic model of the tangential discontinuity magnetopause. This model predicts (1) that not all configurations of magnetic field vectors and magnetosheath velocity allow an equilibrium to exist and (2) that there is a preference for a particular magnetic field rotation sense across the magnetopause due to the different response of ions and electrons to the electric field in the current layer. In the present paper we extend the original model to allow for different magnetospheric and magnetosheath densities and temperatures, and we show that the conclusions remain essentially unchanged. Given the large-scale magnetosheath flow pattern around the magnetosphere, we also compute which regions of the dayside magnetopause may be in tangential discontinuity equilibrium for a given magnetosheath field orientation.

### 1. Introduction

The Earth's magnetic field can be considered, in a first approximation, an impermeable obstacle immersed in the solar wind. The shocked solar wind in the dayside magnetosheath is deflected around the magnetospheric cavity; the interface between both forms the magnetospheric boundary. This boundary corresponds to major changes in the thermal plasma properties as the magnetospheric plasma is tenuous and hot, being typically 5–10 times less dense and 5 times hotter than the magnetosheath plasma [e.g., *Paschmann et al.*, 1993; *Phan and Paschmann*, 1996]. This boundary is also associated with a rotation of the magnetic field from its magnetosheath direction, controlled by the interplanetary magnetic field, to the northward magnetospheric field orientation. The layer that carries the current responsible for this rotation is the magnetopause (MP). The first clear experimental identification of the magnetopause was recorded by a magnetometer aboard Explorer 12 [*Cahill and Amazeen*, 1963]. Usually, a region containing a mixture of magnetosheath and magnetospheric plasma is observed immediately earthward of the magnetopause, forming the so-called low-latitude boundary layer (LLBL) [*Eastman et al.*, 1976]. *Paschmann et al.* [1993] and *Phan and Paschmann* [1996] present average profiles of the magnetic field, the plasma density and the temperature throughout the MP/LLBL region, obtained by superposed epoch analysis of data from Active Magnetospheric Particle Tracer Explorers/Ion Release Module (AMPTE/IRM) magnetospheric boundary layer crossings. They show that the MP/LLBL region is about twice as wide as the magnetopause current layer. The profiles reveal progressive changes of the mag-

netic field and plasma properties from their magnetosheath to magnetospheric values.

Early models [e.g., *Lerche*, 1967; *Davies*, 1969; *Ferraro and Davies*, 1968; *Parker*, 1969] treated the magnetopause as a tangential discontinuity (TD). The importance of the magnetosheath plasma velocity, varying from zero at the stagnation point up to nearly the undisturbed solar wind speed at the flanks, was soon recognized. *Sestero* [1966] envisaged a unidirectional magnetic field in the presence of transverse flow, a configuration representative for the low magnetic shear dawn and dusk magnetopause. He found that the structure of the layer depends on the sense of the flow, an effect due to the electric field inside the layer. For similar configurations, hybrid particle simulations by *Cargill and Eastman* [1991] showed that the length scale of the transition in the bulk velocity profile and, correspondingly, in the ion density profile, changes with the direction of the flow. *Kuznetsova et al.* [1994] suggested an equilibrium TD model that is a combination of the *Harris* [1962] and *Sestero* [1966] models. For a high magnetic shear configuration with a shear velocity parallel or antiparallel to the magnetic field variation, they found that a solution exists for only one of both velocity orientations, suggesting a north-south asymmetry. *De Keyser and Roth* [1997a, b] elaborated a model (henceforth called the "DKR model") that allows arbitrary magnetic field rotation angle and shear flow orientation. They show that TD equilibrium is possible only for particular orientations of the shear flow. The basic idea is illustrated in Figure 1 for the low magnetic shear case. The TD layer is formed by interpenetration of ions and electrons from either side. In general, the ions have the largest gyroradius, so they penetrate farthest onto the opposite side of the TD (Figure 1a). In the presence of shear flow the sense of the flow fixes the sign of the electric field (which is mainly determined by the convection electric field). For the orientation shown in Figure 1b, the electric field pushes the ions in the outer fringes of the TD away from the center of the layer.

Copyright 1998 by the American Geophysical Union.

Paper number 97JA03710.  
0148-0227/98/97JA-03710\$09.00

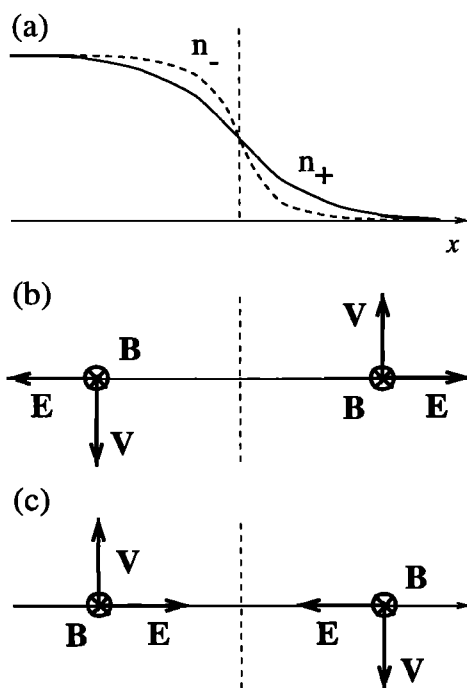


**Figure 1.** The DKR model [De Keyser and Roth, 1997a] predicts the response of ions and electrons in a tangential discontinuity to depend on the sense of the shear flow on either side of the layer. (a) The number densities of protons (solid line) and electrons (dashed line) to the left of the TD gradually vanish across the layer; the densities of protons and electrons on the right side are not shown as they are symmetric with respect to the center of the layer. The protons are expected to penetrate furthest onto the other side of the transition because of their larger gyroradius. (b) In a unidirectional magnetic field  $B$  (pointing inside the paper), one sense of the shear flow  $V$  gives rise to an electric field  $E$  directed away from the center of the layer, which tends to pull the protons in the outer fringes of the TD out of the transition layer. (c) For the opposite flow sense, electrons are pulled out of the layer.

Imagine a thermal ion incident from the left that attempts to cross the layer. It has to traverse a region where the electric field repels it: The layer constitutes an energy barrier. The height of the energy barrier is proportional to the distance over which the ion density vanishes (proportional to the ion gyroradius) and to the electric field (which in turn depends on the shear flow). If the shear flow is too strong, the kinetic energy of the ions is not sufficient to overcome the barrier, and no equilibrium is possible [De Keyser and Roth, 1997a]. Stronger velocity shear can be endured in the opposite flow sense (Figure 1c): because of the smaller electron gyroradius, a larger shear flow is needed to set up an energy barrier for the electrons that prohibits equilibrium. Taking the shear flow across the magnetospheric boundary to be essentially the magnetosheath flow, a magnetic field sense-of-rotation asymmetry is derived from the DKR model.

The DKR model is, up to our knowledge, the first model that predicts the sense and range of magnetic field rotation angles for which TD equilibrium is allowed at any given site

on the magnetopause surface. This result complements the finding of *Su and Sonnerup* [1968] for a wide rotational discontinuity (RD) that the tangential magnetic field component should rotate clockwise from its magnetospheric to its magnetosheath orientation in the northern hemisphere and counterclockwise in the southern hemisphere; that is, the magnetic field rotation has the electron polarization sense of a large-amplitude Alfvén wave. The early Explorer 12 observations [Sonnerup and Cahill, 1968] were in agreement with the wide RD analysis. *Berchem and Russell* [1982b], however, failed to find the predicted relationship using ISEE 1 and 2 data. They conclude that the observed rotation sense is not consistent with the electron whistler polarization theory.

The validity of the DKR model may be questioned since it assumes equal magnetosheath and magnetospheric densities and proton and electron temperatures. The observations (e.g., those presented by *Phan and Paschmann* [1996]) show that this is generally not true; moreover, the magnetosheath and magnetospheric plasmas tend to be very different. In particular, the sharp temperature gradient observed at the magnetopause is expected to give rise to a significant thermoelectric field in addition to the convection electric field, which will alter the structure and behavior of the layer. The purpose of the present paper is (1) to extend the DKR model to include the effects of different magnetospheric and magnetosheath densities and temperatures and (2) to show that the conclusions of the DKR model regarding the magnetic field rotation sense remain essentially valid. The paper focuses on the dayside magnetopause. The particular merit of this paper lies in the adaptation of the DKR model to realistic plasma and magnetic field configurations, thereby paving the way for a direct comparison of the model with satellite observations of the magnetopause current layer. Such a comparison is presented in a companion paper.

## 2. Existence Domains

The DKR model predicts that for a given magnetic field configuration not all plasma velocity jumps across the magnetopause lead to TD equilibrium. In this section we compute the domain of velocity jumps across the magnetopause for which an equilibrium TD configuration exists.

### 2.1. DKR Model

The DKR model describes symmetric transitions (for which  $B^{\text{msph}} = B^{\text{msh}}$ ) with identical plasmas on either side, with the additional assumption that the proton and electron temperatures are equal, that is, equal number densities  $N^{\text{msph}} = N^{\text{msh}}$  and temperatures  $T^{\text{msph}-} = T^{\text{msph}+} = T^{\text{msh}-} = T^{\text{msh}+}$ . The model refers to the particular reference frame introduced in Figure 2: a boundary normal coordinate system rotated around the local magnetopause normal (the  $x$  axis) so that  $y$  becomes the inner bisectrix of the magnetospheric and magnetosheath magnetic field vectors  $B^{\text{msph}}$  and  $B^{\text{msh}}$ . The DKR model is based on a kinetic description of the plasmas in terms of a number of (proton and electron) populations with a prescribed non-Maxwellian ve-

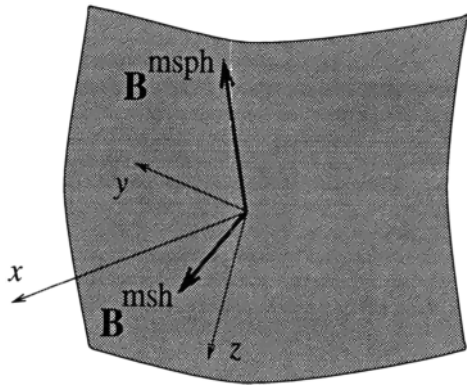


**Figure 2.** The reference frame used in the theoretical analysis by De Keyser and Roth [1997a] is defined as follows:  $x$  is the outward-pointing magnetopause normal,  $y$  is the inner bisectrix of the magnetosheath and magnetospheric magnetic fields  $B^{\text{msh}}$  and  $B^{\text{msph}}$ , and  $z$  completes the right-handed orthogonal set. The  $yz$  plane coincides with the locally planar magnetopause surface.

locity distribution function (VDF). The VDF is chosen such that its moments can be computed analytically [Roth *et al.*, 1996]. Each VDF is parameterized by a so-called transition length  $\mathcal{L}$ , which can be regarded as the scale length of the population density profile inside the magnetopause; its minimum value is one gyroradius  $\rho$  in the uniform field on either side of the transition. De Keyser and Roth [1997a] argue that typically  $\mathcal{L}_- < \mathcal{L}_+$  because of the larger proton gyroradius. At the same time the ratio  $\mathcal{L}_+/\mathcal{L}_-$  should not be too large in order to avoid strong local electric fields associated with charge separation effects inside the transition layer, which might easily initiate instabilities. The values of the transition lengths are further constrained by the magnetopause thickness. The structure of the magnetopause obviously depends on the properties of the magnetospheric and magnetosheath plasmas, but it is also affected by the inner populations, which are confined to the magnetopause current layer and therefore called “trapped” populations [Lee and Kan, 1979]. The inner populations have an overall drift speed that depends on the distance scale  $\mathcal{L}_d$  (a length scale for the width of the  $B_z$  reversal layer that contains the inner particles) by

$$V_d = \frac{2kT}{\mathcal{L}_d eB} = \frac{\rho^+}{\mathcal{L}_d} V_{th}^+,$$

where  $V_{th}^+$  is the proton thermal velocity [Harris, 1962]. Ions and electrons drift in opposite directions, oriented more or less along the  $y$  axis. Given the transition lengths and the magnetic field reversal distance scale, the Vlasov-Maxwell equations (which are reduced to a pair of ordinary differential equations) can be solved numerically.

The DKR model shows that not all bulk velocity jumps  $\mathbf{V}_r = \mathbf{V}^{\text{msh}} - \mathbf{V}^{\text{msph}}$  are compatible with a given magnetic field profile. We can outline the domain of velocity jump vectors for which the model allows TD equilibrium by numerically computing the structure of the transition for each  $\mathbf{V}_r/V_{th}^+$  and checking whether a solution exists that meets

the boundary conditions: uniform magnetic fields on either side of the transition, rotated over a prescribed angle  $\theta_B$ .

Figure 3a shows the domain for a moderate magnetic field rotation  $\theta_B = 90^\circ$  (the overall shape of the existence region does not depend strongly on the precise value of  $\theta_B$ ),  $\beta = 2$ , and  $\mathcal{L}_d = 2\rho^+$ . A reasonable choice for the characteristic transition lengths, compatible with magnetopause thickness observations [e.g., Berchem and Russell, 1982a], is  $\mathcal{L}_- = \rho^+$ ,  $\mathcal{L}_+ = 3\rho^+$ . The existence domain is indicated by the shaded region. This domain is symmetric with respect to the  $V_{rz}$  axis. Its largest extent is for  $V_{rz} < 0$ . An approximate lower bound for the maximum velocity jump magnitude along the  $-V_{rz}$  axis was derived for the DKR model [De Keyser and Roth, 1997a]:

$$|V_{rz}^{\text{max}}| > \frac{2}{\sqrt{\pi}} \left( \frac{1}{\mathcal{L}_-} - \frac{1}{\mathcal{L}_+} \right) \rho^+ V_{th}^+. \quad (1)$$

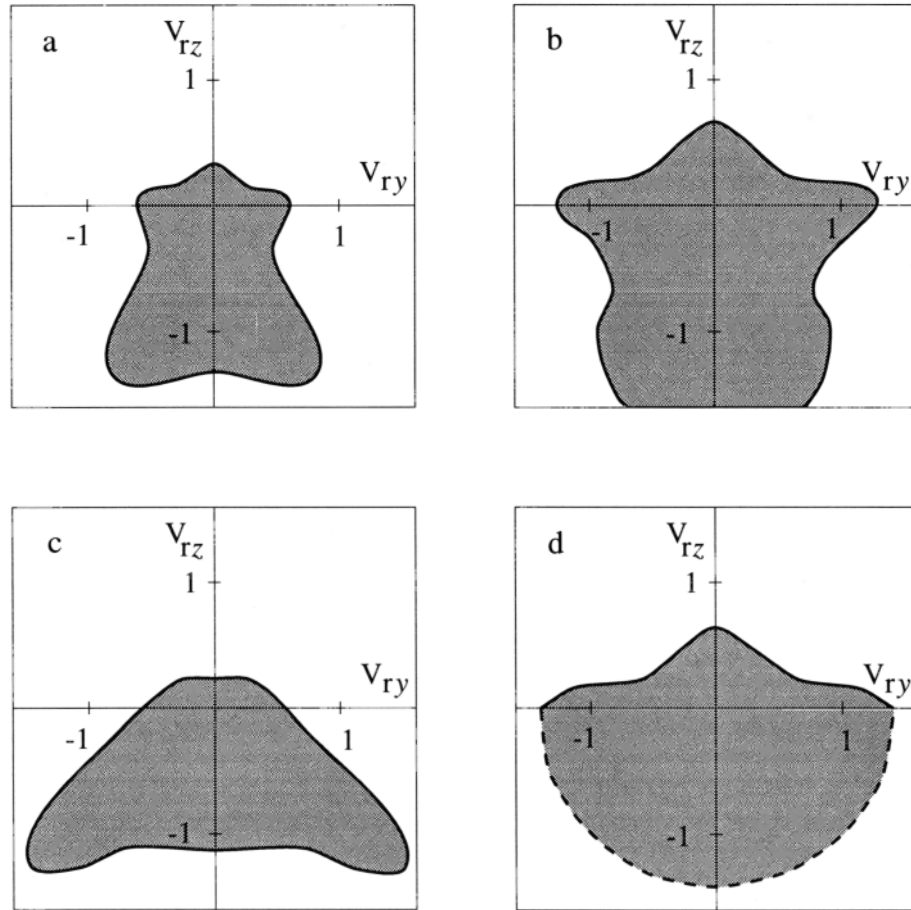
For the characteristic lengths adopted here, this amounts to  $|V_{rz}^{\text{max}}| > 0.75 V_{th}^+$ , consistent with the value  $|V_{rz}^{\text{max}}| \approx 1.20 V_{th}^+$  found from the numerical simulations performed to construct the diagram.

Figure 3b shows the existence domain for smaller transition lengths with the same  $\mathcal{L}_+/\mathcal{L}_-$  ratio ( $\beta = 2$ ,  $\mathcal{L}_- = \frac{2}{3}\rho^+$ ,  $\mathcal{L}_+ = 2\rho^+$ ,  $\mathcal{L}_d = 2\rho^+$ ). The existence domain is larger as expected from (1), which predicts  $|V_{rz}^{\text{max}}| > 2.26 V_{th}^+$ , consistent with  $|V_{rz}^{\text{max}}| \approx 2.68 V_{th}^+$  found from numerical simulation. Figure 3c repeats the diagram of Figure 3a for  $\beta = 4$ , illustrating that the influence of plasma beta is not very pronounced. In general, the existence domain becomes slightly larger when  $\beta$  increases and when the prescribed magnetic field rotation angle  $\theta_B$  decreases. Similar diagrams are found whenever  $\mathcal{L}_+ > \mathcal{L}_-$ , their main property being their large extent along the  $-V_{rz}$  axis. The size of this extent can be estimated from (1), which stresses the importance of the transition lengths. It is now possible to sketch a joint existence domain that represents the superposition of the existence domains for all magnetic field rotation angles, plasma beta conditions, and transition lengths that are expected to occur at the dayside magnetopause. Such a qualitative superposition is shown in Figure 3d. The dashed half circle corresponds to  $V_r/V_{th}^+ \approx 1.4$ , the maximum relative velocity at the dayside magnetopause (a value derived from AMPTE/IRM observations); the precise form of the existence domain outside this circle therefore is of no interest here. We are led to conclude that for  $V_r/V_{th}^+ \gtrsim 0.5$ , equilibrium is possible only when  $V_{rz} < 0$ : the orientation of large velocity jumps is not arbitrary.

## 2.2. Realistic Configurations

The original DKR model assumes the plasmas on either side of the transition to be identical. Of course, this is not the typical situation at the magnetopause. Even in the relatively rare occurrence of symmetric configurations (where  $B^{\text{msph}} = B^{\text{msh}}$ ), plasma densities and temperatures on either side of the transition tend to be different.

We have extended the DKR model in order to account for realistic values of the plasma parameters. First of all, we



**Figure 3.** Bulk velocity jump existence domains (the shaded regions) for symmetric TDs with a transition length ratio  $\mathcal{L}_+/\mathcal{L}_- = 3$  and a magnetic field rotation  $\theta_B = 90^\circ$ : (a) for  $\beta = 2$ ,  $\mathcal{L}_- = \rho^+$ ,  $\mathcal{L}_+ = 3\rho^+$ , and  $\mathcal{L}_d = 2\rho^+$ ; (b) for  $\beta = 2$ ,  $\mathcal{L}_- = \frac{2}{3}\rho^+$ ,  $\mathcal{L}_+ = 2\rho^+$ , and  $\mathcal{L}_d = 2\rho^+$ ; (c) for  $\beta = 4$ ,  $\mathcal{L}_- = \rho^+$ ,  $\mathcal{L}_+ = 3\rho^+$ , and  $\mathcal{L}_d = 2\rho^+$ ; (d) sketched superposition of existence domains for typical transition lengths and plasma beta values. The dashed half circle corresponds to the maximum velocity jump magnitude observed at the dayside magnetopause; the shape of the domain outside this circle is of no interest for the present study. For  $V_r/V_{th}^+ \gtrsim 0.5$ , TD equilibrium appears to be possible only when  $V_{rz} < 0$ .

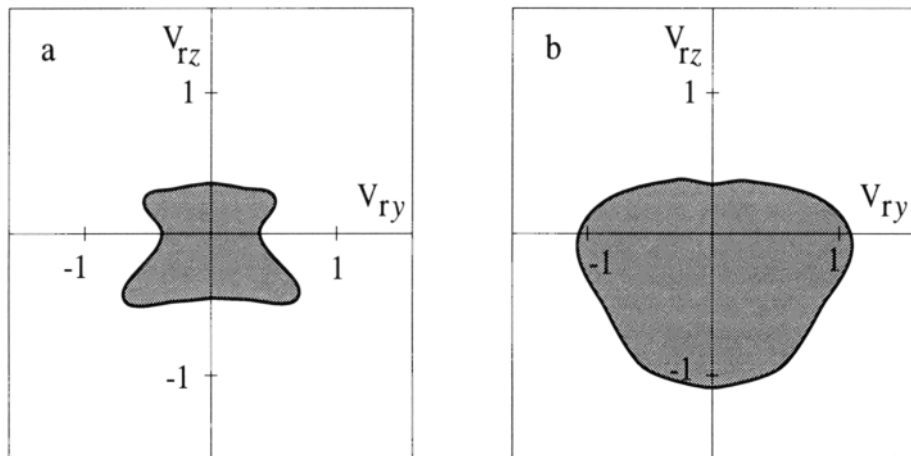


**Figure 4.** Bulk velocity jump existence domains for symmetric TDs with different proton and electron temperatures ( $T^+/T^- = 5$ ,  $\beta = 1.07$ ,  $\mathcal{L}_d = 2\rho^+$ , and  $\theta_B = 90^\circ$ ): (a)  $\mathcal{L}_+ = 3\rho^+$  and  $\mathcal{L}_- = \rho^+$ ; (b)  $\mathcal{L}_+ = 3\rho^+$  and  $\mathcal{L}_- = 0.45\rho^+$ . The latter choice is more appropriate since colder electron populations are expected to have a smaller transition length.

drop the requirement that proton and electron temperatures should be equal. Figure 4 shows the existence domains for transitions with  $T^+/T^- = 5$ , where  $\beta = 1.07$ ,  $\mathcal{L}_d = 2\rho^+$ , and  $\theta_B = 90^\circ$ . Figure 4a shows the case  $\mathcal{L}_+ = 3\rho^+$ ,  $\mathcal{L}_- = \rho^+$ , while Figure 4b corresponds to  $\mathcal{L}_+ = 3\rho^+$ ,  $\mathcal{L}_- = \rho^+/\sqrt{5}$ . The latter choice seems more appropriate: as the gyroradius of colder electrons is smaller, their transition length is expected to be smaller as well. The diagrams confirm that the temperature difference between protons and electrons does not affect the qualitative nature of the existence domains: the preference for  $V_{rz} < 0$  remains an essential characteristic.

We also have extended the DKR model to accommodate for the observed differences between magnetospheric and magnetosheath plasmas and magnetic field strengths. Figure 5 shows the existence domain for a case where  $B^{\text{msph}} = 70$  nT,  $B^{\text{msh}} = 42$  nT,  $N^{\text{msph}} = 2.35 \text{ cm}^{-3}$ ,  $T^{\text{msph}+} = 10^7$  K,  $T^{\text{msph}-} = 2 \times 10^6$  K,  $N^{\text{msh}} = 24.7 \text{ cm}^{-3}$ ,  $T^{\text{msh}+} = 4 \times 10^6$  K, and  $T^{\text{msh}-} = 8 \times 10^5$  K. This corresponds to  $B^{\text{msh}}/B^{\text{msph}} = 0.60$ ,  $\beta^{\text{msph}} = 0.2$ , and  $\beta^{\text{msh}} = 2.3$ . The transition lengths are  $\mathcal{L}_+^{\text{msh}} = 3\rho^{\text{msh}+}$ ,  $\mathcal{L}_-^{\text{msh}} = \rho^{\text{msh}+}/\sqrt{5}$ ,  $\mathcal{L}_+^{\text{msph}} = 3\rho^{\text{msph}+}$ ,  $\mathcal{L}_-^{\text{msph}} = \rho^{\text{msph}+}/\sqrt{5}$ ,  $\mathcal{L}_d^{\text{msh}} = 2\rho^{\text{msh}+}$ , and  $\mathcal{L}_d^{\text{msph}} = 2\rho^{\text{msph}+}$ . Figure 5a shows the existence domain for  $\theta_B = -90^\circ$ , while Figure 5b, its mirror image, is obtained for  $\theta_B = +90^\circ$ . The consequence of the difference in magnetospheric and magnetosheath plasma properties is a deformation of the existence domain; the diagrams for positive and negative rotations no longer are the same. While the existence domain is still largest for  $V_{rz} < 0$ , it now also includes a larger part of the upper quadrants.

### 2.3. Discussion

The influence of the orientation of the velocity jump on the structure and behavior of a tangential discontinuity can be understood from the role of the electric field inside the

layer [e.g., *Sestero*, 1966; *Cargill and Eastman*, 1991; *De Keyser and Roth*, 1997a]: the orientation of the velocity jump with respect to the magnetic field determines the sign of the convection electric field and hence creates an energy barrier for either the protons or the electrons roughly equal to charge times the electric field times the ion or electron transition length in the layer. In the absence of temperature gradients, a difference between the proton and electron transition lengths will cause the height of the energy barriers to differ when the sense of the velocity jump is reversed; the maximum allowed velocity jump will then be different too. Thermoelectric contributions to the electric field may alter the energy barriers, but the convection electric field dominates, especially when the velocity jump is large.

### 3. Magnetic Field Rotation Sense

The predictions of the DKR model regarding the preference for a particular orientation of the magnetic field and the velocity jump can be translated into specific rules for the magnetic field rotation sense at the dayside magnetopause. The magnetospheric magnetic field has a fixed northward orientation. The velocity jump across the MP/LLBL boundary layer can be approximated by the magnetosheath velocity, since the plasma velocity in the magnetosphere or in the LLBL sufficiently far earthward of the magnetopause is relatively small. Given some model of the magnetosheath flow, the existence of a TD equilibrium at a given point on the magnetopause surface then depends only on the magnetosheath magnetic field orientation.

#### 3.1. DKR Model

*De Keyser and Roth* [1997a] consider the consequences of the preferential velocity jump orientation for the high magnetic shear case ( $|\theta_B| \approx 180^\circ$ ) near the noon meridian and the low magnetic shear case ( $|\theta_B| \approx 0^\circ$ ) at the dawnside

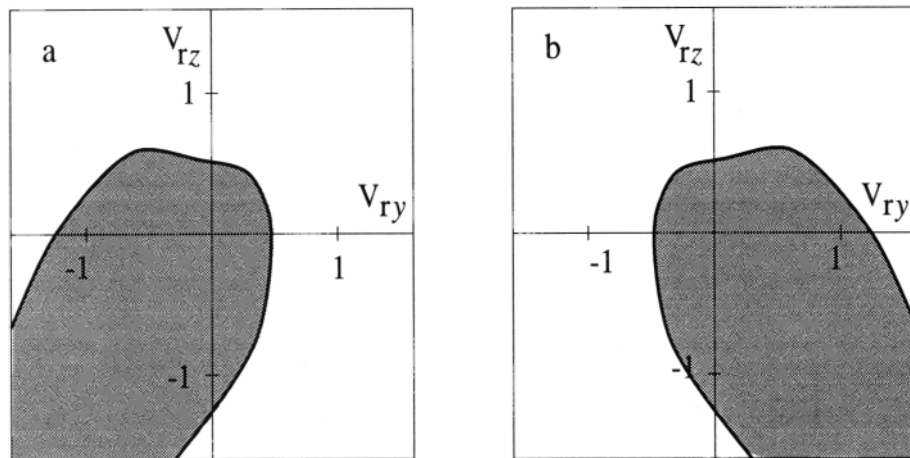


**Figure 5.** Bulk velocity jump existence domains for asymmetric transitions with magnetic field strength, number density, and temperature changes across the magnetopause:  $B^{\text{msph}} = 70$  nT,  $B^{\text{msh}} = 42$  nT,  $N^{\text{msph}} = 2.35 \text{ cm}^{-3}$ ,  $T^{\text{msph}+} = 10^7$  K,  $T^{\text{msph}-} = 2 \times 10^6$  K,  $N^{\text{msh}} = 24.7 \text{ cm}^{-3}$ ,  $T^{\text{msh}+} = 4 \times 10^6$  K, and  $T^{\text{msh}-} = 0.8 \times 10^6$  K. This corresponds to  $\beta^{\text{msph}} = 0.2$  and  $\beta^{\text{msh}} = 2.3$ . The transition lengths are  $\mathcal{L}_+^{\text{msh}} = 3\rho^{\text{msh}+}$ ,  $\mathcal{L}_-^{\text{msh}} = 0.45\rho^{\text{msh}+}$ ,  $\mathcal{L}_+^{\text{msph}} = 3\rho^{\text{msph}+}$ ,  $\mathcal{L}_-^{\text{msph}} = 0.45\rho^{\text{msph}+}$ ,  $\mathcal{L}_d^{\text{msh}} = 2\rho^{\text{msh}+}$ , and  $\mathcal{L}_d^{\text{msph}} = 2\rho^{\text{msph}+}$ . The domains are constructed for (a)  $\theta_B = -90^\circ$  and (b)  $\theta_B = +90^\circ$ .

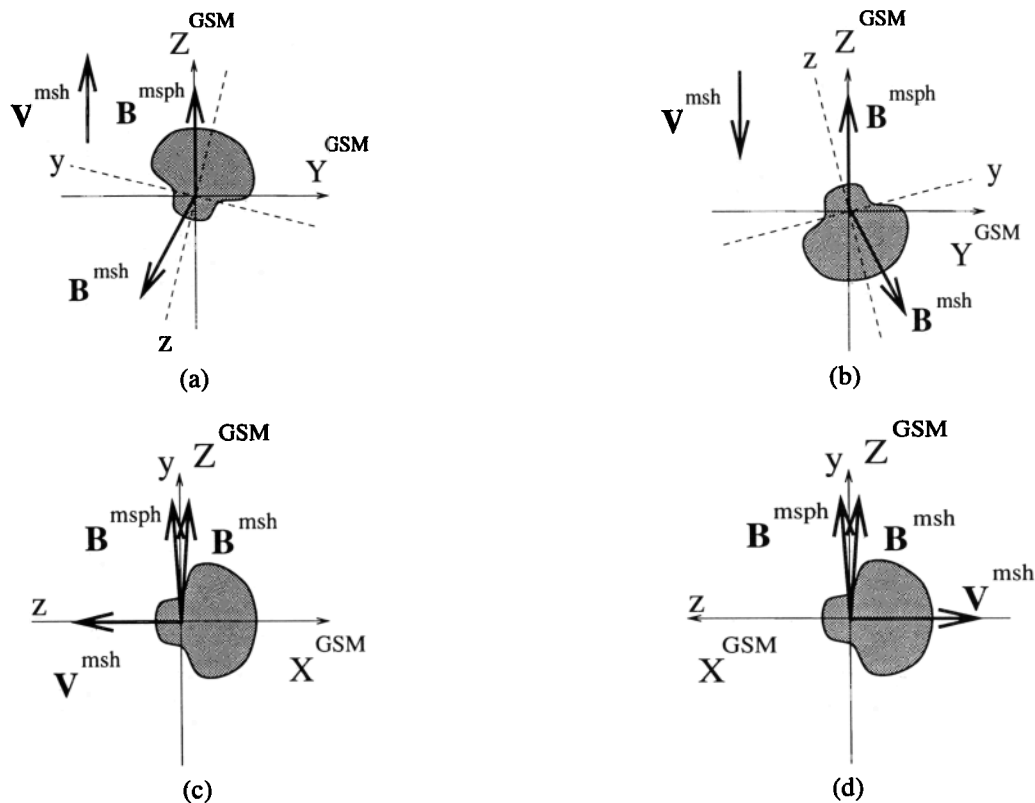


**Figure 6.** Dayside magnetopause configurations: (a) high magnetic shear near the noon meridian, northern latitude, (b) high magnetic shear near the noon meridian, southern latitude, (c) low magnetic shear at the dawnside, and (d) low magnetic shear at the duskside. The figures show the GSM and the  $yz$  frames. The outline of the velocity jump domain is sketched as well as the magnetosheath flow  $V^{msh}$ , which is taken to be representative of the velocity jump across the MP/LLBL layer (adapted from De Keyser and Roth [1997a]).

and the duskside. Figure 6a shows the typical situation for a large positive magnetic field rotation angle near the noon meridian. The  $yz$  frame is drawn in dashed lines; the  $y$  axis is the inner bisectrix of  $B^{msh}$  and  $B^{msph}$ . The typical shape of the existence domain is indicated (the existence domain is constructed in the  $yz$  frame). The  $z$  axis nearly coincides with the  $-Z^{GSM}$  axis. The condition  $V_{rz} < 0$  therefore translates into a condition of northward magnetosheath flow, that is, large positive magnetic field rotation occurs in the northern hemisphere. Figure 6b shows the converse situation, with large negative magnetic field rotation occurring in the southern hemisphere. The situation is peculiar at the dawnside and the duskside for small rotation angle, when the  $z$  axis coincides with the  $Y^{GSM}$  axis: the condition  $V_{rz} < 0$  is never satisfied at the dawnside (Figure 6c), while it is always satisfied at the duskside (Figure 6d).

It is possible to generalize this picture for arbitrary magnetic field rotation angles and arbitrary positions on the dayside magnetopause surface. We take the magnetosheath plasma to stream radially away from the stagnation point. Requiring  $V_r = 0$  at the stagnation point and  $V_r/V_{th}^+ \approx 1.4$  at the dawnside and the duskside (a value derived from low-latitude AMPTE/IRM magnetopause crossings), we adopt the relation

$$V_r/V_{th}^{msh+} \approx 0.016 \alpha,$$

where  $\alpha$  is the angular distance from the stagnation point expressed in degrees. In the previous section it was shown that a typical existence domain might look like the one depicted in Figure 7a: for  $V_r/V_{th}^+ < 0.5$  any velocity jump orientation is allowed, while for larger velocities only  $V_{rz} < 0$  leads to TD equilibrium. It is then possible to predict which regions on the dayside magnetopause surface correspond to equilibrium TD configurations for a given magnetic field rotation angle  $\theta_B$ . In Figures 7b–7f these regions are indicated by shading on a GSM plot of the dayside magnetopause, for magnetic field rotation angles of  $+180^\circ$ ,  $+90^\circ$ ,  $0^\circ$ ,  $-90^\circ$ , and  $-180^\circ$ ; these sketches were prepared while putting the stagnation point  $5^\circ$  downward from the stagnation point, for zero dipole tilt angle.

A common characteristic of these plots is the circular region around the stagnation point, where the magnetosheath velocity is small enough so that no preferential orientation, and hence no preference for a particular sense of rotation, is present. Farther away from the stagnation point, however, only half of the remaining surface allows an equilibrium. Figures 7b and 7f illustrate that there is a north–south asymmetry for high magnetic shear ( $|\theta_B| \approx 180^\circ$ ). Figure 7d illustrates the conclusion that no equilibrium is possible at the dawnside for low magnetic shear ( $|\theta_B| \approx 0^\circ$ ). As explained in Figure 6c, the velocity jump vector has the wrong orientation

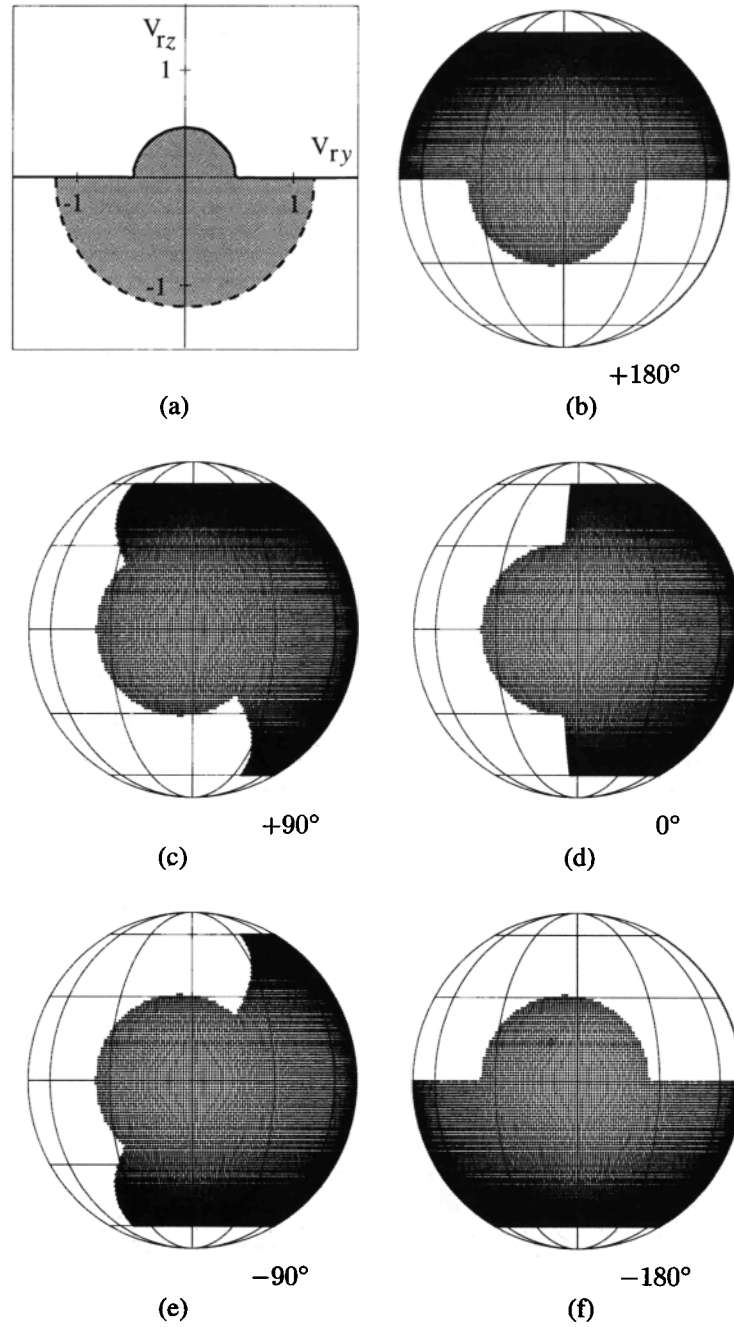


**Figure 7.** Given the velocity jump vector domain for symmetric transitions, and assuming that the magnetosheath plasma is streaming radially away from the stagnation point, the DKR model permits the dayside magnetopause to be in TD equilibrium for a given magnetic field rotation angle only in certain regions. (a) Velocity jump vector domain. (b) The shaded region indicates where TD equilibrium can exist for a magnetic field rotation angle of  $+180^\circ$ , (c)  $+90^\circ$ , (d)  $0^\circ$ , (e)  $-90^\circ$ , and (f)  $-180^\circ$ . The stagnation point is taken to be located  $5^\circ$  downward from the subsolar point. The dipole tilt angle is zero.

tation: TD equilibrium appears impossible, at least for the transition length values adopted here. Only high magnetic shear configurations can be in a state of TD equilibrium at the dawnside.

### 3.2. Realistic Configurations

As discussed in the previous section, the DKR model is modified when more realistic values for the plasma param-

eters are considered. Figure 8 qualitatively sketches the modified existence regions corresponding to plasma asymmetries like those in Figure 5. The global picture remains unchanged. There now appears to be a band around the dawnside equator where both large positive and negative rotations may be present. But, again, it appears impossible to obtain TD equilibrium at the dawnside for small rotation angle.

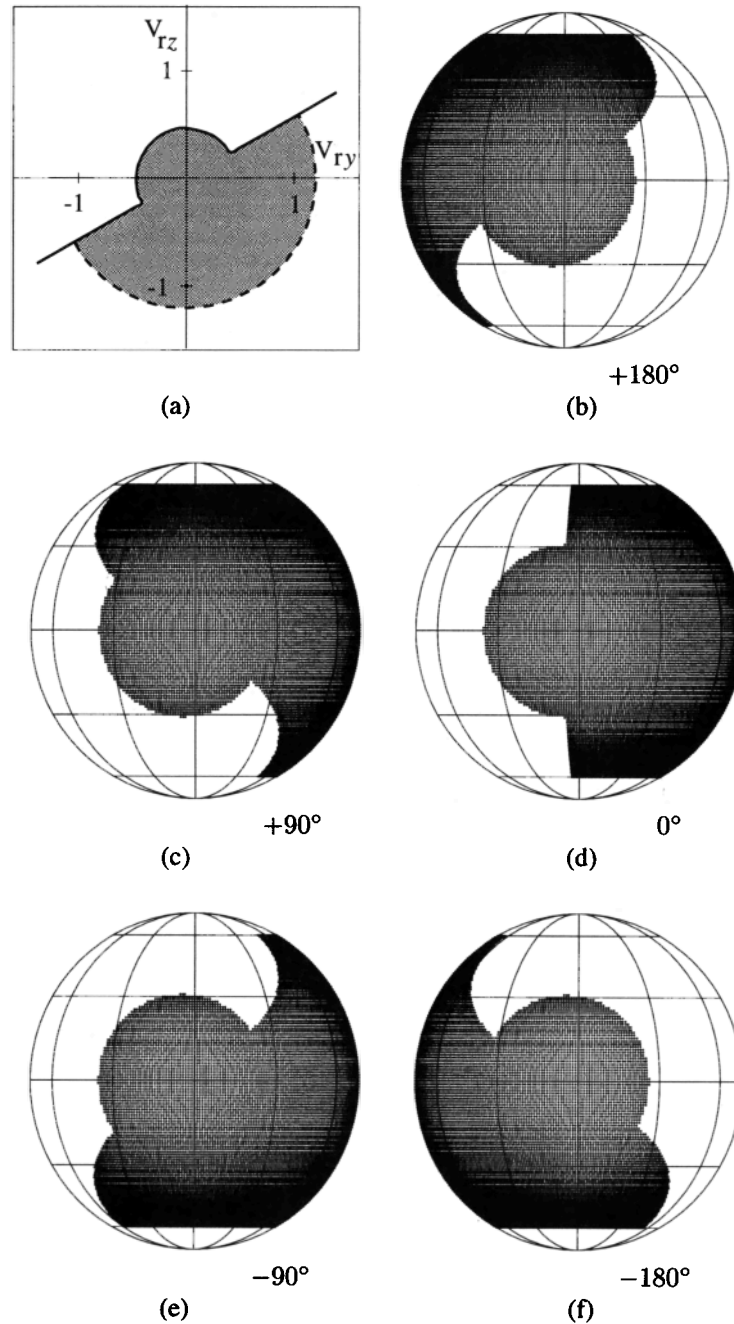


**Figure 8.** The same as Figure 7 but now for typical asymmetric transitions. (a) Velocity jump vector domain with a shape that depends on the magnetic field rotation angle; the sketch shown here corresponds to a large positive rotation (see also Figure 5). (b) The shaded region indicates where TD equilibrium can exist for a magnetic field rotation angle of  $+180^\circ$ , (c)  $+90^\circ$ , (d)  $0^\circ$ , (e)  $-90^\circ$ , and (f)  $-180^\circ$ .

### 3.3. Discussion

Figures 7 and 8 are only sketches that illustrate the overall consequences of the DKR model. Tilt angle variations, deviations from the adopted relation between shear flow and stagnation point distance, fluctuations in the location of the stagnation point, and variations in the magnetosheath beta will in effect blur the demarcation lines between regions where TD equilibrium may exist and where it may not.

We can summarize the conclusions as follows: (1) any

magnetic field rotation is allowed near the stagnation point, (2) there is a tendency for large positive rotations to occur predominantly in the northern hemisphere, (3) large negative rotations are expected predominantly in the southern hemisphere, (4) small positive and negative rotations are possible at the duskside, and (5) no low magnetic shear TD equilibrium seems possible at the dawnside. It is interesting to note that the north-south asymmetry of the rotation sense for high magnetic shear TDs is the same as the one predicted by the electron whistler polarization theory for wide RDs [Su and Sonnerup, 1968].

We want to stress that the plots of Figures 7 and 8 should not be considered as snapshots of the magnetopause at any given instant, since  $\theta_B$  usually differs from place to place on the magnetopause surface. In the present study we have made no attempt to relate the magnetic field orientation in the magnetosheath adjacent to the magnetopause to the interplanetary magnetic field direction in the preshock region.

#### 4. Conclusions

This paper was devoted to a study of the magnetic field rotation sense at the dayside magnetopause from a theoretical point of view. The predictions of the DKR model [De Keyser and Roth, 1997a, b] have been further elaborated and generalized in order to account for realistic plasma and magnetic field properties at the magnetopause.

The first part of this study dealt with the relationship between the magnetic field configuration and the velocity jump across the magnetopause. The DKR model predicts, for TDs interfacing plasmas with identical density and temperature, that not all velocity jump vectors allow an equilibrium that is compatible with a given magnetic field configuration to exist. We have extended the DKR model by computing existence domains also for realistic plasma conditions by including the effects of density and temperature gradients. The predictions of the DKR model remain essentially unchanged: for large velocity jumps there are constraints on the orientation of the velocity jump with respect to the magnetic field.

In the second part of the paper we used our knowledge of the shape of the existence domain to identify the regions on the dayside magnetopause where TD equilibrium is possible for a given magnetic field rotation angle. The general picture is (1) there is no preference for a particular rotation sense near the stagnation point, (2) large positive magnetic field rotations predominantly occur in the northern hemisphere, (3) large negative rotations occur mostly in the southern hemisphere, (4) both positive and negative low magnetic shear crossings may occur near the duskside, and (5) no low magnetic shear TD equilibrium is possible at the dawnside.

The particular merit of this paper lies in extending the DKR model for more realistic plasma parameters. The conclusions regarding the magnetic field rotation sense have been cast in a form that allows the model to be confronted with in situ observations. The overall picture is more complicated than the *Su and Sonnerup* [1968] theory. It is tempting to compare our predictions with the ISEE observations reported by *Berchem and Russell* [1982b]. As *Berchem and Russell* [1982b, Figure 4] show only the magnetic field rotation sense (not the rotation angle) and present their results in the GSE frame (rather than the GSM frame), an overall comparison is not possible. Among the specific examples shown by *Berchem and Russell* [1982b, Figure 2] there is one dawnside crossing, at 0740 magnetic local time (MLT) and  $-22^\circ$  magnetic latitude (MLAT); it has a high magnetic shear (about  $150^\circ$ ) and a negative sense of rotation, which is consistent with the DKR model. Both the *Berchem and Russell* results and the DKR model reject the electron whistler polarization rule. To test the DKR model predictions further,

we have examined a number of AMPTE/IRM magnetopause crossings; we have found no TD crossing that did not satisfy the existence conditions derived from the DKR model. These results are presented in a companion paper.

The DKR model asserts that, in certain circumstances, the magnetopause cannot be in TD equilibrium. What is the state of the magnetopause then? We suggest three possibilities: (1) the magnetopause may become another type of discontinuity, for example, a rotational discontinuity; (2) the magnetopause may become macroscopically unstable, for example, the Kelvin-Helmholtz instability might occur; (3) microinstabilities (turbulence) may develop. The three possibilities imply some form of plasma transport across the magnetospheric boundary.

This paper addressed the overall velocity difference between the large-scale magnetosheath flow and the magnetospheric or LLBL plasma. Localized high-speed tangential flows inside the LLBL (often taken to be the signature of reconnection [e.g., *Sonnerup et al.*, 1981; *Phan et al.*, 1996]) may exist but have not been considered here.

The inner populations, the particles actually carrying the diamagnetic current responsible for the magnetic field rotation at the magnetopause, play a key role in theoretical models [see, e.g., *Whipple et al.*, 1984]. Nevertheless, not much is known about their origin or precise distribution. The hypotheses that are made about them in the DKR model follow previous studies [e.g., *Harris*, 1962; *Roth et al.*, 1996].

We made no attempt in this paper to relate the magnetic field configuration at the magnetopause to the interplanetary magnetic field conditions. Such a study would have to include a study of the bow shock and the magnetosheath as well and would be an important step toward a global understanding of the magnetosphere.

**Acknowledgments.** The authors thank B. T. Tsurutani, E. N. Parker, J. F. Lemaire, and D. Hubert for stimulating discussions, and D. Sibeck for helpful comments on the manuscript. Part of the work described in this paper was performed at the Belgian Institute for Space Aeronomy under a PRODEX contract with ESA in the framework of the Ulysses Interdisciplinary Study on Directional Discontinuities. We acknowledge the support of the Belgian Federal Services for Scientific, Technical and Cultural Affairs.

The Editor thanks Timothy E. Eastman and another referee for their assistance in evaluating this paper.

#### References

- Berchem, J., and C. T. Russell, The thickness of the magnetopause current layer: ISEE 1 and 2 observations, *J. Geophys. Res.*, **87**, 2108–2114, 1982a.
- Berchem, J., and C. T. Russell, Magnetic field rotation through the magnetopause: ISEE 1 and 2 observations, *J. Geophys. Res.*, **87**, 8139–8148, 1982b.
- Cahill, L. J., and P. G. Amazeen, The boundary of the geomagnetic field, *J. Geophys. Res.*, **68**, 1835–1843, 1963.
- Cargill, P. J., and T. E. Eastman, The structure of tangential discontinuities, 1, Results of hybrid simulations, *J. Geophys. Res.*, **96**, 13,763–13,779, 1991.
- Davies, C. M., The structure of the magnetopause, *Planet. Space Sci.*, **17**, 333–338, 1969.
- De Keyser, J., and M. Roth, Equilibrium conditions for the tangential discontinuity magnetopause, *J. Geophys. Res.*, **102**, 9513–9530, 1997a.

- De Keyser, J., and M. Roth, Correction to "Equilibrium conditions for the tangential discontinuity magnetopause," *J. Geophys. Res.*, *102*, 19,943, 1997b.
- Eastman, T. E., E. W. Hones Jr., S. J. Bame, and J. R. Asbridge, The magnetospheric boundary layer: Site of plasma, momentum and energy transfer from the magnetosheath into the magnetosphere, *Geophys. Res. Lett.*, *3*, 685–688, 1976.
- Ferraro, V. C. A., and C. M. Davies, Discussion of paper by E. N. Parker, "Confinement of a magnetic field by a beam of ions," *J. Geophys. Res.*, *73*, 3605–3606, 1968.
- Harris, E. G., On a plasma sheath separating regions of oppositely directed magnetic field, *Nuovo Cimento*, *23*, 115–121, 1962.
- Kuznetsova, M. M., M. Roth, Z. Wang, and M. Ashour-Abdalla, Effect of the relative flow velocity on the structure and stability of the magnetopause current layer, *J. Geophys. Res.*, *99*, 4095–4104, 1994.
- Lee, L. C., and J. R. Kan, A unified kinetic model of the tangential magnetopause structure, *J. Geophys. Res.*, *84*, 6417–6426, 1979.
- Lerche, I., On the boundary layer between a warm, streaming plasma and a confined magnetic field, *J. Geophys. Res.*, *72*, 5295–5310, 1967.
- Parker, E. N., Solar wind interaction with the geomagnetic field, *Rev. Geophys.*, *7*, 3–10, 1969.
- Paschmann, G., W. Baumjohann, N. Sckopke, T.-D. Phan, and H. Lühr, Structure of the dayside magnetopause for low magnetic shear, *J. Geophys. Res.*, *98*, 13,409–13,422, 1993.
- Phan, T. D., and G. Paschmann, Low-latitude dayside magnetopause and boundary layer for high magnetic shear, 1, Structure and motion, *J. Geophys. Res.*, *101*, 7801–7815, 1996.
- Phan, T. D., G. Paschmann, and B. U. Ö. Sonnerup, Low-latitude dayside magnetopause and boundary layer for high magnetic shear, 2, Occurrence of magnetic reconnection, *J. Geophys. Res.*, *101*, 7817–7828, 1996.
- Roth, M., J. De Keyser, and M. M. Kuznetsova, Vlasov theory of the equilibrium structure of tangential discontinuities in space plasmas, *Space Sci. Rev.*, *76*, 251–317, 1996.
- Sestero, A., Vlasov equation study of plasma motion across magnetic fields, *Phys. Fluids*, *9*, 2006–2013, 1966.
- Sonnerup, B. U. Ö., and L. J. Cahill, Explorer 12 observations of the magnetopause current layer, *J. Geophys. Res.*, *73*, 1757–1770, 1968.
- Sonnerup, B. U. Ö., G. Paschmann, I. Papamastorakis, N. Sckopke, G. Haerendel, S. J. Bame, J. R. Asbridge, J. T. Gosling, and C. T. Russell, Evidence for magnetic field reconnection at the Earth's magnetopause, *J. Geophys. Res.*, *86*, 10,049–10,067, 1981.
- Su, S.-Y., and B. U. Ö. Sonnerup, First-order orbit theory of the rotational discontinuity, *Phys. Fluids*, *11*, 851–857, 1968.
- Whipple, E. C., J. R. Hill, and J. D. Nichols, Magnetopause structure and the question of accessibility, *J. Geophys. Res.*, *89*, 1508–1516, 1984.

---

J. De Keyser and M. Roth, Belgian Institute for Space Aeronomy, Ringlaan 3, B-1180 Brussels, Belgium. (e-mail: Johan.DeKeyser@oma.be)

(Received July 10, 1997; revised October 15, 1997; accepted October 20, 1997.)